



ELSEVIER

Available online at www.sciencedirect.com

SciVerse ScienceDirect

Proceedings of the Combustion Institute 34 (2013) 1537–1544

Proceedings
of the
Combustion
Institute

www.elsevier.com/locate/proci

Effect of a homogeneous combustion catalyst on combustion characteristics of single droplets of diesel and biodiesel

Mingming Zhu, Yu Ma, Dongke Zhang*

Centre for Energy (M473), The University of Western Australia, 35 Stirling Highway, Crawley, WA 6009, Australia

Available online 29 June 2012

Abstract

Combustion characteristics of single droplets of diesel and biodiesel in air at temperatures between 923 K and 1073 K, with and without being dosed with a ferrous picrate based homogenous combustion catalyst, were studied. The time-resolved ignition and burnout behaviour of the droplets were observed with the aid of a CCD camera, which enabled the determination of the ignition delay period, the burnout time and the flame temperature using the thermal imaging taken by the CCD camera. A flame emission spectrometer was used for identification of the presence of iron ions in the flame and TGA experiments were carried out to study the thermal decomposition behaviour of pure ferrous picrate. It was found that the catalyst shortened the burnout time, increased the burning rate and the flame temperature of the droplets of both diesel and biodiesel. At the catalyst dosing ratio of 1:10,000 (by volume) in the diesel and biodiesel, the flame temperatures of the catalyst dosed droplets were about 40–50 K higher than those of the droplets without the catalyst while the burning rate was 0.05–0.1 mm² s⁻¹ higher. It was also found that the biodiesel droplets had longer ignition delay period but shorter burnout times, higher burning rates and flame temperatures than those of the diesel droplets. Iron ions were detected to present in the flame of the combustion of the catalyst droplet alone and it was found that the pure ferrous picrate decomposed at 523 K. This low decomposition temperature of the picrate ensured the release of the iron ions into the flame, which in turn promoted the combustion rate of the fuel vapour.

© 2012 The Combustion Institute. Published by Elsevier Inc. All rights reserved.

Keywords: Biodiesel; Combustion characteristics; Diesel; Droplets; Homogeneous combustion catalyst

1. Introduction

Compression ignition (CI) engines fuelled with diesel, commonly known as diesel engines, play an important role in modern society. Due to ever rising petroleum price and increasingly more stringent emission regulations, there is a continuing

need to develop alternative technologies to utilize diesel in a more efficient and cleaner manner [1]. The application of homogeneous combustion catalysts in diesel engines is one such promising technique, among others, to achieve higher engine efficiency and lower emissions [2].

One type of the homogeneous combustion catalysts is organo-metallic compounds [2,3], which play a catalytic role during diesel combustion in engines. They are added into diesel in tiny amounts at ppm levels to form a stable, uniform mixture.

* Corresponding author. Fax: +61 8 6488 7235.

E-mail address: Dongke.Zhang@uwa.edu.au (D. Zhang).

The addition of such homogeneous combustion catalysts does not change the physical properties of diesel and no modifications to the engines are required. A number of metal ions have been found to promote diesel combustion such as Iron [4], Cerium [5], Platinum [6], Copper [7], and Manganese [8]. The effects of some homogeneous combustion catalysts on the performance of diesel engines fuelled with biodiesel have also been studied [8,9]. Biodiesel, converted from vegetable oil or animal tallow, has been promoted by its proponents as an alternative fuel for its claimed benefits of lower greenhouse gas emissions and lower sulphur concentrations [10]. It has been reported that the use of manganese and iron based catalysts could improve the physical properties of biodiesel and reduce the brake specific fuel consumption (BSFC) and engine emissions [8,9]. However, the majority of studies of homogeneous combustion catalysts found in the literature have focused on the performance of diesel engines, including the authors own recent work [11,12], and little scientific attention has been devoted to the mechanisms of the catalysts in the combustion processes.

A series of studies into a ferrous picrate based homogeneous combustion catalyst has been enacted in the authors' laboratories. The composition of the catalyst is a ferrous picrate–water–butanol solution with additives [2]. These additives are mainly short-chain alkyl benzene and its derivatives, which help improve the stability of the ferrous picrate–water–butanol–diesel mixture [2]. Based on laboratory tests using a small diesel engine [11,12], BSFC was improved by up to 4.2% and the smoke emission was reduced by 25% with the addition of the catalyst in diesel. However, the mechanisms of the catalyst in the diesel combustion process remain unclear. Diesel combustion in CI engines is very complex, involving compression of combustion air, fuel injection, evaporation and mixing, and ignition and complex chemical reactions (combustion) between the fuel vapour and air. The complexity of such complex chemical and physical processes makes it difficult to single out the effect of the homogeneous catalysts in diesel combustion to be studied at the mechanistic level.

Against this backdrop, an experimental study of ignition and burnout behaviour of single droplets of diesel and biodiesel, with and without being dosed with the homogeneous combustion catalyst, was performed in order to understand the mechanisms of the catalyst. This present contribution details this work and its findings.

2. Experimental

2.1. Materials

A commercial diesel (Caltex No.2 diesel), a biodiesel provided by Bioworks Australia Pty

Ltd., and a ferrous picrate catalyst manufactured by Fuel Technology Pty Ltd., were used for experimentation. The Fe^{2+} content in the catalyst was within the range of 560–600 mg L⁻¹ and the catalyst was added into diesel and biodiesel at dosing ratios of 1:20,000, 1:10,000, 1:5000 and 1:2000 by volume, respectively. The specifications of diesel, biodiesel and the catalyst are listed in Table 1. Analysis of the catalyst dosed fuels showed that the addition of the catalyst at all dosing ratios had no observable effect on the physical properties, including density, viscosity, flash point, cloud and pour point, as well as colour, of both diesel and biodiesel.

2.2. Experimental procedures

The single droplet ignition and combustion experiments of diesel and biodiesel were carried out in the apparatus as illustrated in Fig. 1a. This experimental configuration was first used by Faeth and Olsen [13] and then widely used by other researchers for ignition delay studies [14]. The experimental setup consisted of a horizontal tube furnace with temperature control for providing a hot air environment, a droplet suspension system, a step motor for delivering the droplet into the furnace and a CCD camera for measuring the ignition delay period, total burnout time and flame temperature.

The experiments were performed in air at temperatures between 923 and 1073 K, in which a diesel droplet was ignited and combusted. The temperature of the furnace (550 mm in length, 40 mm in diameter) was regulated using the temperature controller with an accuracy of ± 1 K. A droplet was produced by a micro-syringe of 10 μL in volume and deposited on the tip of a quartz fibre of approximately 200 ± 10 μm in diameter.

The droplet suspended on the fibre was delivered into the isothermal zone at the centre of the furnace with the aid of the step motor at a linear velocity of 1 ms⁻¹, which allowed about 0.15 s for the droplet to reach the furnace centre. The high speed CCD camera (Basler PIA-210gc) was used to capture the images of the process from the moment when the droplet entered the furnace till it burned out completely, at a frame rate of 200 fs⁻¹ (exposure time 0.25 ms) to enable adequate determination of the ignition delay period and total burnout time. For recording the evolution of the droplet sizes during combustion, the camera was backlit by a 50 W halogen lamp. A computer was used to operate the step motor and the CCD camera.

A flame emission spectrometer was applied to detect iron ions in the flame of the pure catalyst, and the diesel and the biodiesel dosed with the catalyst. Figure 1b shows the schematic diagram of the system. The spectrometer (StellarNet, BLACK-Comet-XR) permitted the acquisition of spectra

Table 1

Main chemical components and physical properties of the biodiesel, diesel and catalyst.

Species	Component ^a	mol% ^a	Density (g/ml) (15 °C)	Boiling point (K)	Viscosity, cSt (40 °C)	Flash point (K)	Cetane number
Biodiesel	(C ₁₅ H ₃₁)COOCH ₃	18.95%					
	(C ₁₇ H ₃₅)COOCH ₃	5.96%					
	(C ₁₇ H ₃₃)COOCH ₃	41.98%	0.878	478–716	3.42	373	57.1
	(C ₁₇ H ₃₁)COOCH ₃	23.89%					
	(C ₁₇ H ₂₉)COOCH ₃	2.78%					
Diesel	<C10	8.71%					
	C10–C18	75.07%	0.845	473–673	2.02	348	50.1
	>C18	16.22%					
Catalyst			0.876	413–483		316	

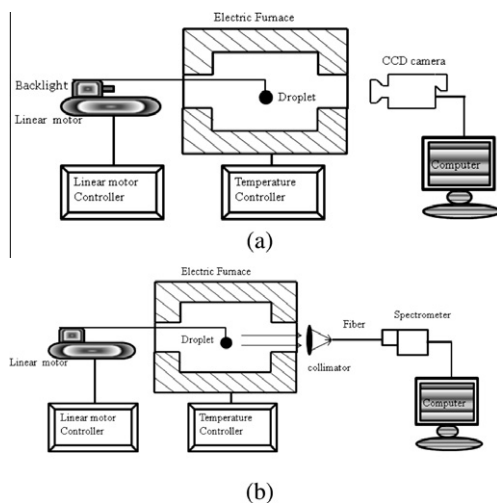
^a From GC–MS analysis.

Fig. 1. A schematic diagram of the apparatus for the droplet combustion experiments (a) with a CCD camera for determination of ignition delay period, burnout time and burning rate and (b) with a flame emission spectroscopy for identification of the presence of iron ions in the flame.

in the wavelength range from 280 to 900 nm with a resolution of 1.5 nm. The spectral energy was transmitted to the monochromator through a fibre optic cable, which was terminated with a collimator. Iron has a very rich line spectrum spanning from the near-ultraviolet to the near-infrared regions [15]. This method can provide a simple and quick qualitative means of determining the presence of iron ions in the flame.

To understand the path that the ferrous picrate undergoes during the diesel combustion process, thermal decomposition of the pure ferrous picrate was carried out using a thermo-gravimetric analyser (TA Instrument SDT Q600). A ceramic crucible was used to hold the sample. The sample (15 mg of ferrous picrate) was heated to 1273 K at a heating rate of 20 K min⁻¹ in air.

2.3. Data analyses

Using the optical images taken by the CCD camera, the ignition delay period, burnout time and the flame temperature were calculated. The ignition delay period (t_i) was defined as the time from the moment the droplet entering the furnace to the moment the first visible flame occurring with an accuracy of 1/200 s. The burnout time (t_c) was defined as the time period between the instance when the droplet was ignited and the completion of the droplet combustion.

The flame temperature was determined using the two-colour pyrometry [16] by analysing the optical spectra from the visual thermal imaging taken by CCD camera [16,17]. This method has been recently adopted to calculate the temperature of sooty flame using the pixel intensity of the images taken by a CCD camera. The principles of this method have been well documented elsewhere [16,17]. A burning droplet was surrounded by an envelope flame with a bright flame zone. In the present study, the flame temperature used in the proceeding discussion refers to the average temperature of the flame zone. All flame temperatures were calculated from at least five repeated measurements. Figure 2 shows a typical diffusion flame of a burning droplet and the calculated temperature distribution.

The back-lighted images of a droplet surrounded by a luminous flame were recorded and post-processed so that the evolution of the droplet size (d_s) during combustion was determined. The post-processing of the images consisted of a super-resolution reconstruction [18] and canny edge detection methods [19], which allowed the edge of a burning droplet to be identified accurately. The actual shape of the suspended droplet in the present experimentation was elliptical due to the influence of gravity and a stated droplet size referred to an equivalent value determined as the cubic root of the product of the droplet width squared and the droplet length [20,21]. The droplet size used in this study was 1.05 ± 0.02 mm.

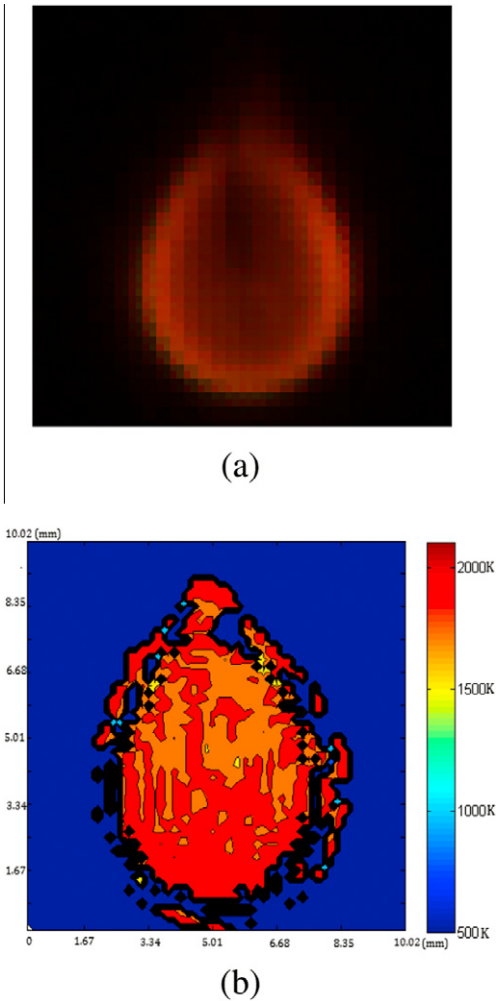


Fig. 2. Typical images of a droplet flame (a) and the associated flame temperature contour (b).

Due to the finite resolution of identification of the boundary that yielded an error of 1 pixel, the inherent uncertainty in calculating the droplet diameter was estimated to be around 2% for the droplet in the present study. Once the time history of the droplet size was known, the burning rate was determined based on the classical d^2 -law of droplet combustion [22]. From the d^2-t plot, the burning rate constant was determined as $k = -d(d_s^2)/dt$.

3. Results and discussion

3.1. Ignition delay period and burnout time

Figure 3 shows the effect of the catalyst dosing ratio on the ignition delay period of both diesel and biodiesel droplets. It is seen that the addition

of the catalyst did not result in any significant difference of the ignition delay period measurable using the present technique. One possible reason is that the effect of the catalyst on the ignition delay period might have been blurred by the inherent measurement error of about 5 ms in the present study.

It is however clear that the ignition delay period of the biodiesel was higher than that of the diesel. This is obviously due to the differences in the chemical compositions between the two fuels and the associated boiling points (Table 1). Table 1 shows that biodiesel has a higher Cetane number than that of diesel, which is consistent with the literature [23]. However, Cetane number measures the ignition quality of diesel spray into a hot and high pressure environment, which cannot be used to explain the results in the current studies. The ignition delay period of droplets consists of droplet heating, molecular diffusion/mixing and gas phase chemical reaction, in which the droplet heating plays a significant role. The boiling points of the biodiesel are higher than those of the diesel (Table 1). When subjected to the same air temperature, the higher boiling point of the biodiesel requires a longer time to heat up and evaporate for combustion. Therefore, the presence of the double bonds in the biodiesel and its higher boiling points are responsible for the longer ignition delay period, with or without the addition of the catalyst.

Figure 4 shows the effect of the catalyst dosing ratio on the burnout time of both diesel and biodiesel droplets. It is seen that the burnout times of droplets were reduced significantly by the addition of the catalyst. The burnout time decreased with increasing the catalyst dosing ratio but this effect levelled off when the catalyst dosing ratio was greater than 1:5000. It is also evident that the biodiesel had a slightly shorter burnout time com-

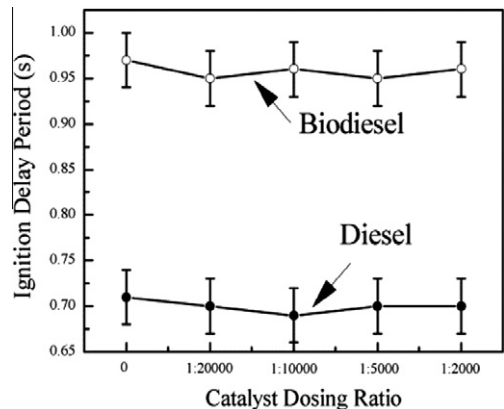


Fig. 3. Effect of the catalyst dosing ratio on the ignition delay period of both diesel and biodiesel droplets at 973 K.

pared to the diesel fuel, which may be explained by the higher oxygenate content and therefore a higher burning rate for biodiesel.

3.2. Burning rate

Figure 5 plots the temporal variations of the square of droplet diameter (d_s) after ignition, for both diesel and biodiesels with and without the catalyst at different ambient temperatures. The d^2 -law [22] dictates that the square of the droplet diameter decreases linearly with time. It is evident from Fig. 5 that the d^2 -law [22] is well conformed to by the burning droplets after an initial period of heating. This conformation is more profound at higher temperatures. At the higher temperatures, the ignition delay period was so short that the bulk temperature of the droplet is far below the boiling temperature upon the occurrence of the ignition and continued to increase after the ignition until reaching the boiling point. At lower temperatures, the droplet size of the biodiesel at ignition was greater than that of the diesel although the initial droplet sizes were the same. This observation confirms that the biodiesel droplets evaporated at a slower rate, due to its higher boiling points, than the diesel before ignition.

Figure 6 compares the burning rates of diesel and biodiesel with the catalyst at different temperatures. It is seen that the burning rates of both fuels increased with increasing temperature. It is also evident that the catalyst enhanced the burning rates of both fuels. For example, at 973 K, the burning rate increased from 0.83 mm²/s to 0.88 mm²/s for the diesel and from 0.97 mm²/s to 1.06 mm²/s for the biodiesel, respectively, when the catalyst was added at a 1:10,000 dosing ratio. However, when the catalyst dosing ratio doubled, the burning rate did not increase proportionally. This is in accordance with the observation of the effect of the catalyst on the burnout time (Fig. 4).

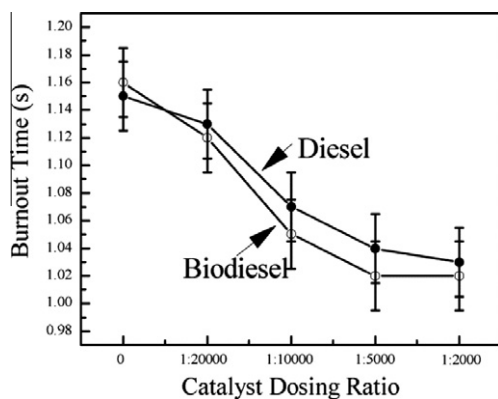


Fig. 4. Effect of the catalyst dosing ratio on the burnout time of both diesel and biodiesel droplets at 973 K.

From Fig. 6, it was found that the burning rate of the biodiesel droplet was higher than that of the diesel. This is due to the oxygenate content in the biodiesel fuel.

3.3. Flame temperature

The effect of the catalyst on flame temperature is shown in Fig. 7. Figure 7a shows the measured instantaneous flame temperatures, as a function of time, for the droplets of pure diesel and diesel dosed with the catalyst at 1:10,000 and 1:5000 ratios at 973 K. The flame temperatures reached a very high point, more than 2400 K, immediately after ignition, and then decreased sharply to level off at a constant value during steady burning of the droplet, and, in the final stage of the combustion process, gradually decreased towards the end. This corresponds to the two phases of droplet combustion in which the premixed combustion of the fuel vapour involved in the auto-ignition phase and the mixing-controlled diffusion flame of the fuel vapour in the steady burning of the droplets. The combustion of the diesel and biodiesel droplets at other temperatures exhibited the same trend.

Figure 7b illustrates the flame temperatures during the steady burning of the droplets of both diesel and biodiesel dosed with the catalyst at the dosing ratios of 1:10,000 and 1:5000, at various temperatures. The flame temperatures increased as the furnace temperature increased. The flame temperatures of the droplets dosed with the catalyst were higher than those of the pure fuels, respectively. At 973 K, the flame temperatures of the diesel and biodiesel droplets rose around 40 K with the catalyst dosing ratio of 1:10,000. However, when the catalyst dosing ratio doubled from 1:10,000 to 1:5000, the flame temperature only further increased by approximately 10 K, or 50 K over the flame temperatures of the pure fuels. The flame temperatures of the biodiesel droplets were about 30–50 K higher than those of the diesel at the same temperatures. The higher burning rate is thought to be responsible for the increased flame temperature, which in turn increased the burning rate of the biodiesel droplets, as shown in Fig. 6.

Regardless the fuel type, the addition of the catalyst increased the flame temperatures, which is considered to be due to (1) enhanced burning rate of the fuel vapour and (2) reduced radiation heat loss from the flames as less soot was formed in the combustion.

3.4. Mechanisms of the catalytic effect

The preceding discussion has shown that the use of the ferrous picrate based homogeneous catalyst reduced the burnout times, enhanced the burning rate and increased flame temperatures

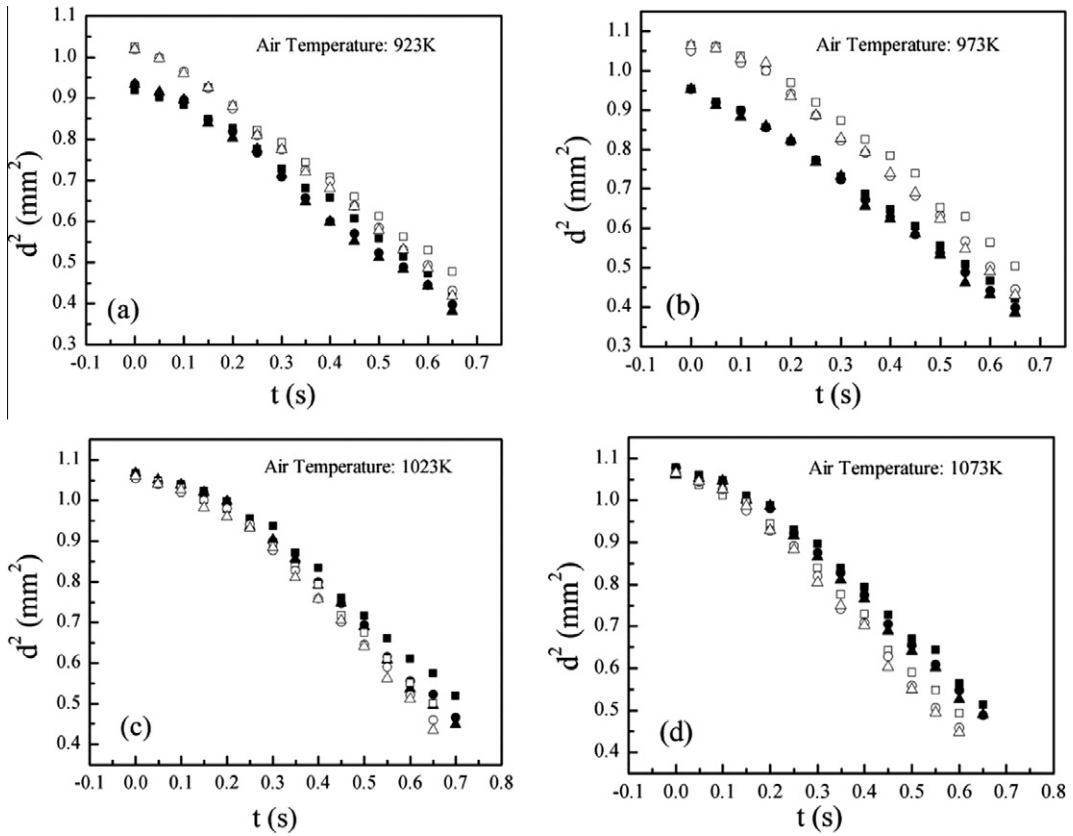


Fig. 5. The d^2 - t plots for burning droplets of diesel and biodiesel with and without the catalyst at different temperatures. ■: diesel; ●: diesel dosed with the catalyst at a dosing ratio of 1:10,000; ▲: diesel dosed with the catalyst at a dosing ratio of 1:5000; □: biodiesel; ○: biodiesel dosed with the catalyst at a dosing ratio of 1:10,000; △: biodiesel dosed with the catalyst at a dosing ratio of 1:5000.

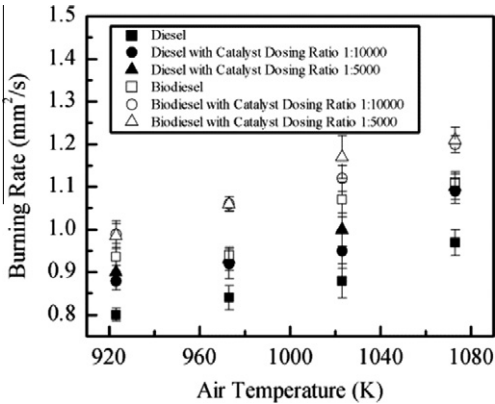


Fig. 6. Burning rates of diesel and biodiesel droplets with and without the catalyst at different temperatures.

of droplets of both diesel and biodiesel. In order to understand the mechanisms of the ferrous picrate in the combustion process, the flame emission

spectroscopy and thermo-gravimetric analysis of ferrous picrate were conducted. The flame emission spectroscopy was used for identification of the presence of iron ions in the flame and the TGA experiments were carried out to find out the decomposition temperature of the pure ferrous picrate.

Figure 8 illustrates the emission spectra of the flames of the pure catalyst. The spectra showed all possible light emissions ranging from 280 nm to 900 nm during the combustion process and a spectrum with major feature near 589.1 nm, which corresponds to one of the atomic emission lines for iron [15]. This line spectrum was not found in the flames of the catalyst solvent with the ferrous picrate removed. This suggested that, during combustion of the catalyst, the ferrous picrate decomposed and released iron atom into the luminous flame.

Figure 9 shows the behaviour of thermal decomposition of the pure ferrous picrate. It is seen that the decomposition started at around 473 K at a very slow rate but the vigorous gravimetric

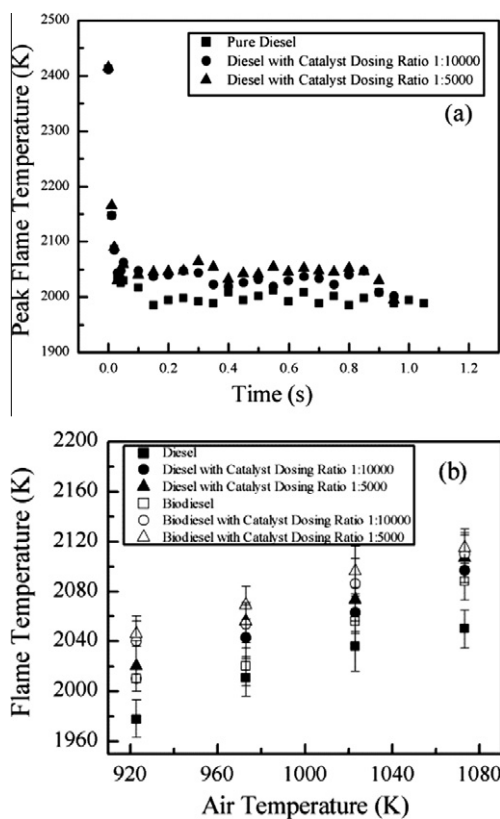


Fig. 7. Flame temperatures of diesel droplets as a function of time at 973 K (a) and flame temperature during quasi-steady combustion of diesel and biodiesel droplets with and without the catalyst at different temperatures (b).

change occurred at 523 K, which was the decomposition temperature of the ferrous picrate under the tested conditions. The results of flame emission spectroscopy and the TGA suggested that the ferrous picrate could decompose at 523 K and released iron atoms upon the decomposition.

Based on the evidence presented above, the mechanism of the ferrous picrate in the combustion process of diesel and biodiesel has been proposed as follows. Table 1 shows that the boiling points of both diesel and biodiesel were higher than the decomposition temperature of ferrous picrate (523 K). When subjected to heat, the surface temperature of the fuel droplets increased till reaching their boiling points. When the surface temperatures of the droplets of the fuels dosed with the catalyst was higher than 523 K, the ferrous picrate decomposed and released iron atoms into the reaction zone, which promoted the oxidation of the fuel vapour. This resulted in higher reaction rates and an increase in the flame temperatures of the catalyst dosed droplets. Consequently, the heat transfer to the droplet was

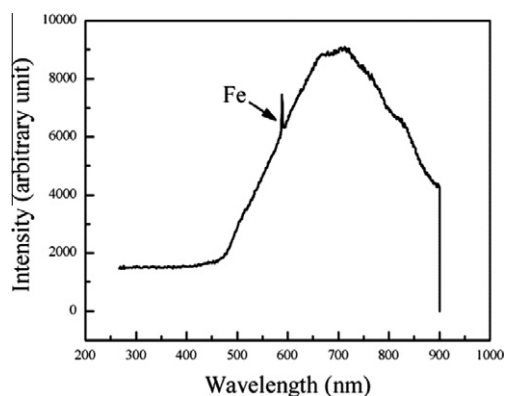


Fig. 8. Flame emission spectra of a burning catalyst droplet at 973 K.

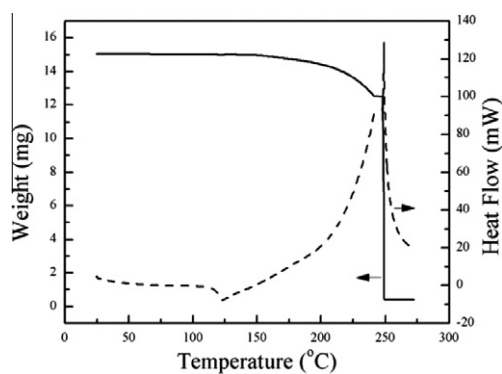


Fig. 9. DSC-TG curves showing the thermal decomposition behaviour of ferrous picrate in air in TGA at a heating rate of 20 K min⁻¹.

enhanced by the higher flame temperature, resulting in a higher burning rate and shorter burnout time. This is consistent with literature reports that atomic iron promotes ignition and combustion of hydrocarbons [24], hydrogen [25] and carbon monoxide [26] at temperatures ranging from 1000 K to 2500 K.

It may also be speculated that, due to the presence of the C–NO₂ bond in ferrous picrate, NO and/or NO₂ released from the ferrous picrate decomposition upon heating may have promoted the ignition and combustion of the fuel droplets. It has been reported that the major N component released during thermal composition of picrate salts is NO instead of NO₂ [27]. It has also been widely recognized that NO, at concentrations of tens to few hundred ppm, was only effective in promoting the oxidation of hydrocarbons at low temperatures [28]. In the present work, the amount of the picrate dosed into the fuels was in the order of several hundred ppb and, assuming all N in the

picrate was converted to NO, the additional NO in the flame due to picrate decomposition would be ca 200 ppb, insufficient to be responsible for the enhanced combustion of the catalyst dosed fuels. Therefore, the promotion effect of ferrous picrate in the high temperature combustion process of the diesel and biodiesel droplets cannot be attributed to NO from the picrate but the iron ions. The tiny amount of catalyst added in the fuels also suggested that the increased flame temperatures measured were not due to the radiation from the iron atoms.

4. Conclusions

A comprehensive study of the effect of the ferrous picrate based homogeneous combustion catalyst on the combustion characteristics of single droplets of diesel and biodiesel has been carried out. It was found that the catalyst shortened the burnout time, increased the burning rate and the flame temperature of diesel and biodiesel droplets. Such effect was enhanced with increasing the catalyst dosing ratio but levelled off when the catalyst dosing ratio was greater than 1:5000. At the dosing ratio of 1:10,000 in the diesel and biodiesel, the flame temperatures of the catalyst dosed droplets were about 40–50 K higher than those of droplets without the catalyst while the burning rate was 0.05–0.1 mm²/s higher.

It was also found that the ferrous picrate decomposed at 523 K and iron ions were detected in the flame of the catalyst droplets alone. It was proposed that the ferrous picrate decomposed and released iron ions into the flame zone during the combustion process of the droplets. The combustion rate was enhanced with the presence of iron ions in the flame, resulting in a higher flame temperature. Consequently, the heat transfer between the flame front and the droplet surface and the evaporation rate were improved.

It was also shown that biodiesel had a longer ignition delay period but a shorter burnout time, higher burning rate and flame temperature than those of diesel. It is assumed that the presence of double bond and oxygen in the biodiesel may be the major factor leading to this difference.

Acknowledgment

This project is supported by the Australia Research Council under the ARC Linkage Projects Scheme (Project Number: LP0989368) in partnership with Fuel Technology Pty Ltd. and BHPBilliton Iron Ore Pty Ltd.

References

- [1] J.E. Dec, *Proc. Combust. Inst.* 32 (4) (2009) 1–16.
- [2] D.K. Zhang, Seventh Asia-Pacific Conference on Combustion, Taiwan, 2009.
- [3] J.B. Howard, J. William, J.R. Kausch, *Prog. Energy Combust. Sci.* 6 (1980) 263–276.
- [4] J.B. Parsons, G.J. Germane, *SAE Technical Paper:* 831204, 1983.
- [5] G. Wakefield, X.P. Wu, M. Gardener, B. Park, S. Anderson, *Technol. Anal. Strategic Manage.* 20 (1) (2008) 127–136.
- [6] D.T. Kelso, W.R. Epply, M.L. Hart, *Fuel Process. Technol.* 91 (3) (2010) 313–321.
- [7] H. Chen, B. Li, B. Zhang, *SAE Technical Paper:* 901492, 1990.
- [8] A. Keskin, M. Guru, D. Altiparmk, *Fuel* 86 (2003) 1139–1143.
- [9] G.R. Kannan, R. Karvembu, R. Anand, *Appl. Energy* 88 (2011) 3694–3703.
- [10] T.X. Li, D.L. Zhu, N.K. Akafuah, K. Saito, C.K. Law, *Proc. Combust. Inst.* 33 (2011) 2039–2046.
- [11] M.M. Zhu, Y. Ma, D.K. Zhang, *Energy* 36 (2011) 6004–6009.
- [12] M.M. Zhu, Y. Ma, D.K. Zhang, *Appl. Energy* 91 (2012) 166–172.
- [13] G.M. Faeth, D.R. Olsen, *SAE Technical Paper:* 680465, 1968.
- [14] A.J. Marchese, T.L. Vaughn, K. Kroenlein, F.L. Dryer, *Proc. Combust. Inst.* 33 (2011) 2021–2030.
- [15] J.E. Sansonetti, W.C. Martin, *J. Phys. Chem. Ref. Data* 34 (4) (2005) 1559–2259.
- [16] H.R. Ma, R. Stevens, R. Stone, *SAE Technical Paper:* 06P-551, 2005.
- [17] M.M. Zhu, H. Zhang, G.T. Tang, et al., *Proc. Combust. Inst.* 32 (2) (2009) 2029–2035.
- [18] N.R. Shah, A. Zakhor, *IEEE Trans. Image Process.* 8 (6) (1999) 879–885.
- [19] J. Canny, *IEEE Trans.* 8 (1986) 679–689.
- [20] D.L. Dietrich, J.B. Haggard, F.L. Dryer, V. Nayar, B.D. Shaw, F.A. Williams, *Proc. Combust. Inst.* 26 (1996) 1201–1207.
- [21] W. Xu, M. Ikegami, S. Honma, et al., *Fuel* 82 (2003) 319–330.
- [22] C.K. Law, *Prog. Energy Combust. Sci.* 8 (3) (1982) 171–201.
- [23] G.A. Ban-Weiss, J.Y. Chen, B.A. Buchholz, R.W. Dibble, *Fuel Process. Technol.* 88 (2007) 659–667.
- [24] K. Park, G.T. Bae, K.S. Shin, *Bull. Kor. Chem. Soc.* 23 (2) (2002) 175–176.
- [25] G.T. Linteris, V.I. Babushok, *Proc. Combust. Inst.* 32 (2) (2009) 2535–2542.
- [26] S. Li, X.L. Wei, *Energy Fuels* 25 (2011) 967–974.
- [27] T.B. Brill, T.L. Zhang, B.C. Tappan, *Combust. Flame* 121 (2000) 662–670.
- [28] Y.L. Chan, F.J. Barnes, J.H. Bromly, A.A. Konnov, D.K. Zhang, *Proc. Combust. Inst.* 33 (2011) 441–447.